

Cannabinoid Receptor Type 1 Modulates Alcohol-Induced Liver Fibrosis

Eleonora Patsenker,^{1*} Matthias Stoll,^{2,6*} Gunda Millonig,³ Abbas Agaimy,⁴ Till Wissniowski,² Vreni Schneider,¹ Sebastian Mueller,³ Rudolf Brenneisen,⁵ Helmut K Seitz,³ Matthias Ocker,^{2,6†} and Felix Stickel^{1†}

¹Department of Clinical Pharmacology and Visceral Research, University of Bern, Switzerland; ²Department of Medicine, University Hospital Erlangen, Germany; ³Center of Alcohol Research, Liver Disease and Nutrition, University of Heidelberg, Germany; ⁴Department of Pathology, University Hospital Erlangen, Germany; ⁵Department of Clinical Research, University of Bern, Switzerland; and ⁶Institute for Surgical Research, Philipps University Marburg, Germany

The cannabinoid system (CS) is implicated in the regulation of hepatic fibrosis, steatosis and inflammation, with cannabinoid receptors 1 and 2 (CB1 and CB2) being involved in regulation of pro- and antifibrogenic effects. Daily cannabis smoking is an independent risk factor for the progression of fibrosis in chronic hepatitis C and a mediator of experimental alcoholic steatosis. However, the role and function of CS in alcoholic liver fibrosis (ALF) is unknown so far. Thus, human liver samples from patients with alcoholic liver disease (ALD) were collected for analysis of *CB1* expression. *In vitro*, hepatic stellate cells (HSC) underwent treatment with acetaldehyde, H₂O₂, endo- and exocannabinoids (2-arachidonoylglycerol (2-AG) and Δ^9 -tetrahydrocannabinol (THC)), and CB1 antagonist SR141716 (rimonabant). *In vivo*, *CB1* knockout (KO) mice received thioacetamide (TAA)/ethanol (EtOH) to induce fibrosis. As a result, in human ALD, *CB1* expression was restricted to areas with advanced fibrosis only. *In vitro*, acetaldehyde, H₂O₂, as well as 2-AG and THC, alone or in combination with acetaldehyde, induced *CB1* mRNA expression, whereas CB1 blockage with SR141716 dose-dependently inhibited HSC proliferation and downregulated mRNA expression of fibrosis-mediated genes *PC α 1(I)*, *TIMP-1* and *MMP-13*. This was paralleled by marked cytotoxicity of SR141716 at high doses (5–10 μ mol/L). *In vivo*, *CB1* knockout mice showed marked resistance to alcoholic liver fibrosis. In conclusion, *CB1* expression is upregulated in human ALF, which is at least in part triggered by acetaldehyde (AA) and oxidative stress. Inhibition of CB1 by SR141716, or via genetic knock-out protects against alcoholic-induced fibrosis *in vitro* and *in vivo*.

© 2011 The Feinstein Institute for Medical Research, www.feinsteininstitute.org

Online address: <http://www.molmed.org>

doi: 10.2119/molmed.2011.00149

INTRODUCTION

Liver fibrosis is a common complication of many chronic liver diseases due to alcohol abuse, chronic hepatitis B and C, nonalcoholic steatohepatitis, prolonged drug exposure and autoimmune causes (1). Upon chronic injury, liver parenchyma is replaced by excess extracellular matrix (ECM) produced by activated hepatic stellate cells (HSC) and myofibroblasts, resulting in cirrhotic remodeling, progressive functional impair-

ment and—potentially—hepatocellular cancer (2–4).

The endocannabinoid system (ECS) comprises endocannabinoids such as arachidonoyl ethanolamide (anandamide, AEA) and 2-arachidonoylglycerol (2-AG), their corresponding receptors (cannabinoid receptors 1 and 2 [CB1 and CB2]) and certain phytocannabinoids such as Δ^9 -tetrahydrocannabinol (THC). Recently, an important role of ECS in liver fibrogenesis was described (5). Upregula-

tion of the ECS in several types of chronic liver damage, but not in healthy liver was demonstrated (6,7). Here, *CB1* expression was confined to activated myofibroblasts and vascular endothelium, whereas *CB2* was expressed by inflammatory cells (8). *CB1* and *CB2* seem to mediate opposite effects in fibrogenesis, as *CB1* knockout mice (*CB1*^{-/-}) are resistant to fibrogenesis induced by CCl₄ thioacetamide (TAA) or bile duct ligation (BDL) (9), whereas *CB2*^{-/-} mice reveal more progressive fibrosis after CCl₄ treatment (10). In addition, pharmacological inhibition of CB1 with rimonabant, a CB1 antagonist, reduced expression of transforming growth factor β 1 (TGF β 1) and α -smooth muscle actin (α SMA), and improved histology of BDL-, TAA- or CCl₄-treated mice (8,9). Clinically, patients with chronic hepatitis C and daily canna-

*EP and MS have contributed equally and share premier authorship; †MO and FS have contributed equally and share senior authorship.

Address correspondence and reprint requests to Felix Stickel, University of Bern, Department of Clinical Pharmacology and Visceral Research, Murtenstr. 35, 3010 Bern Switzerland. Phone: +41 31 632 87 15; Fax: +41 31 632 49 97; E-mail: felix.stickel@ikp.unibe.ch.

Submitted April 21, 2011; Accepted for publication August 18, 2011; Epub (www.molmed.org) ahead of print August 19, 2011.

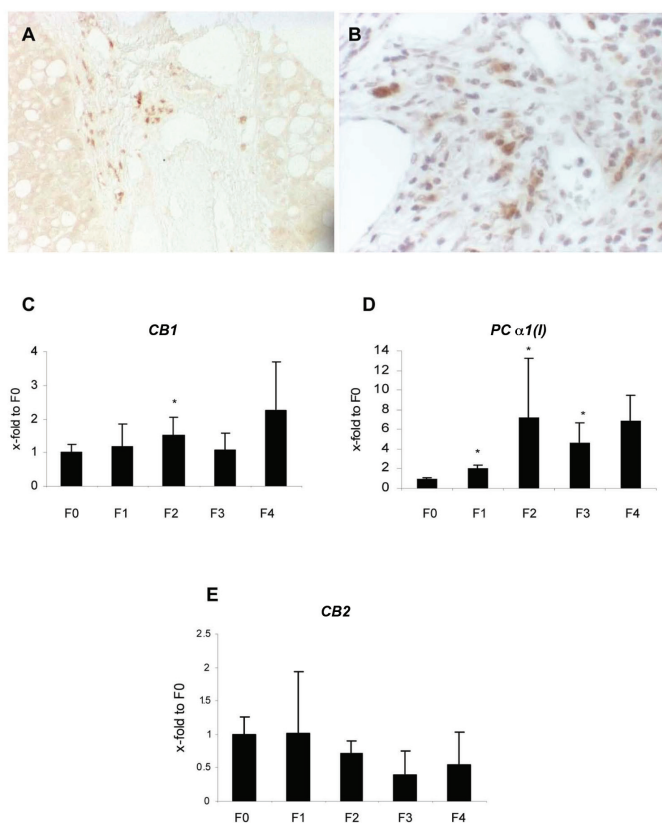


Figure 1. *CB1* and *CB2* expression in human ALD. *CB1* immunohistochemistry performed in paraffin-embedded human liver tissues from patients with ALD. Strong *CB1* positivity can be observed within fibrotic septa (brown color), whereas parenchyma remained negative (A: magnification 10 \times ; B: magnification 40 \times). Shown are representative images. (C) *CB1*, (D) *PCα1(I)* and (E) *CB2* mRNA from liver biopsies of ALD patients with different fibrosis stage, measured by TaqMan PCR and normalized to *GAPDH* (mean \pm SD; **P* < 0.05).

bis consumption displayed more severe fibrosis progression than non- or occasional consumers (11–13).

Endocannabinoid expression is faint in patients with healthy livers, whereas in cirrhosis, fatty liver, acute hepatitis or bile duct obstruction, hepatic and serum levels of AEA and 2-AG were found increased (14–17). Endocannabinoids exert numerous and sometimes opposite effects on liver target cells which could be CB receptor-dependent or independent, and are involved in control of cell survival and apoptosis (18). Thus, AEA induced cell necrosis via several mechanisms, whereas 2-AG induced apoptosis in HSC (10,19,20).

Jeong *et al.* recently found *CB1*^{-/-} mice to be resistant to the steatogenic effects

of alcohol (21), while the opposite effect was observed in *CB2*^{-/-} mice (22). The latter study also investigated the effects of 35 wks of alcohol at 16% in drinking water on fibrosis in mice deficient for either *CB1*^{-/-} or *CB2*^{-/-}. Authors demonstrated HSC activation and increased collagen production in all groups after prolonged ethanol intake, with the strongest effect observed in *CB2*^{-/-} mice, and to a lesser extent in *CB1*^{-/-} mice. In addition to antifibrotic and antisteatotic effects toward alcohol, *CB2* also alleviated hepatic inflammation as evidenced by enhanced inflammatory scores on histology and increased mRNA expression of tumor necrosis factor- α , interleukin-1 β and monocyte chemoattractant protein-1. The protective effect of patent

CB2 receptor status and its activation toward alcohol-mediated liver injury was further underscored by showing that mice fed an alcoholic liquid diet containing 6.2% of alcohol (28% of total calories), and treated with a *CB2* agonist shifted their Kupffer cell response toward a M2-type of pattern favoring resolution of inflammation and wound healing (23). However, the extent of and effects on fibrosis by *CB1* antagonism in the study by Trebicka *et al.* were small, albeit significant, which could be due to the animal model in which mice received alcohol via drinking water. This approach is considered suboptimal with regard to studying aspects of fibrosis since mice are notoriously resistant to profibrogenic effect from alcohol without additional hepatotoxic triggers (24). None of the studies focusing on the role of ECS in the evolution of alcohol-mediated fibrosis have included human samples, or attempted to decipher mechanisms underlying this interaction. Therefore, we aimed to explore the endocannabinoid-dependent mechanisms of alcohol-induced liver injury in human ALD, in experimental alcohol-induced liver fibrosis using *CB1*^{-/-} mice, and in HSC to increase our understanding on how alcohol interacts with *CB1*.

MATERIAL AND METHODS

Human Tissues

Paraffin-embedded and frozen human liver tissues were obtained from consecutive patients with ALD who underwent liver biopsy for diagnostic reasons. Patients consumed at least 80 g/day of alcohol, were predominantly male (74%), had a mean age of 49 \pm 7.4 years and a mean BMI of 25 \pm 3.5 kg/m². Histologically normal liver tissue specimens from patients undergoing abdominal surgery for reasons unrelated to liver disease served as controls. The extent of alcoholic liver injury was scored according to Kleiner *et al.* (25). Liver biopsy specimens used for gene expression revealed the following fibrosis stages: F0, n = 6; F1, n = 6; F2, n = 7; F3, n = 5; F4, n = 3.

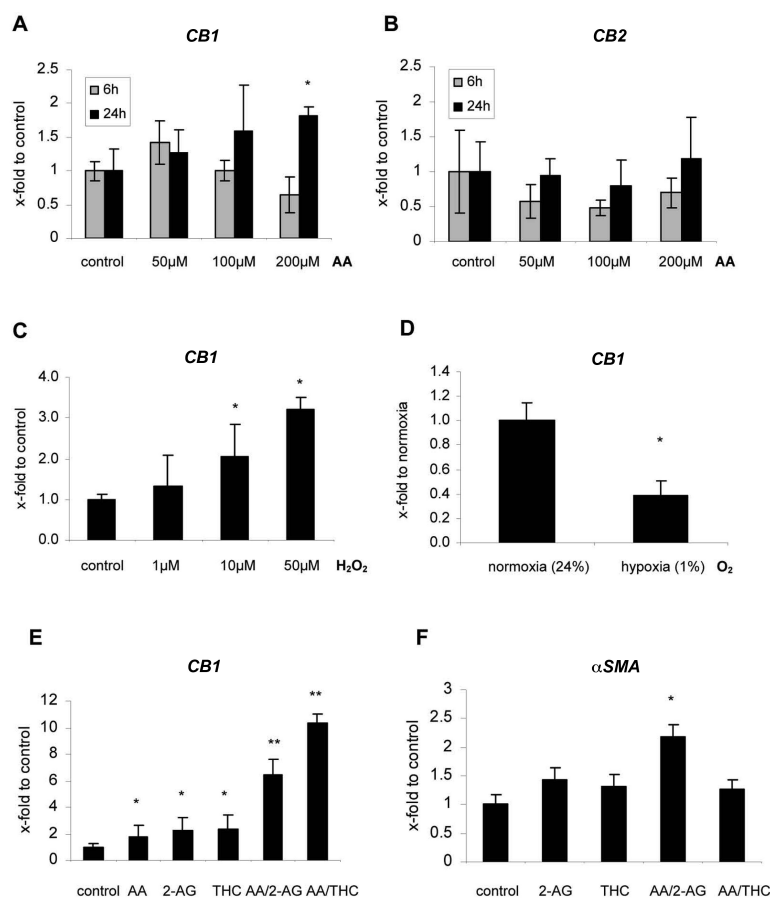


Figure 2. The effect of acetaldehyde, H_2O_2 , hypoxia and endo- and exocannabinoids on *CB1* and fibrosis-related mRNA in HSC. (A) *CB1* and (B) *CB2* mRNA after the treatment with 50–200 $\mu\text{mol/L}$ of acetaldehyde (AA) (6 and 24 h) (human HSC). (C) *CB1* mRNA after the treatment with 1–50 $\mu\text{mol/L}$ H_2O_2 (24 h), (D) *CB1* mRNA under hypoxic conditions (1% O_2) (24 h), (E) *CB1* mRNA after 24 h treatment with 2-AG (20 $\mu\text{mol/L}$) or THC (1 $\mu\text{mol/L}$) alone, or in combination with AA (200 $\mu\text{mol/L}$), and (F) αSMA mRNA after 24 h treatment with 2-AG (20 $\mu\text{mol/L}$) or THC (1 $\mu\text{mol/L}$) alone, or in combination with AA (200 $\mu\text{mol/L}$) (rat HSC); measured by TaqMan PCR and normalized to *GAPDH* (mean \pm SD; * $P < 0.05$, ** $P < 0.005$).

The human study was approved by the Ethics Committee of the University of Heidelberg, Germany where all liver biopsies were collected. All patients gave written informed consent to have their tissues included in the study.

Animal Model

CB1^{-/-} mice and wild-type littermates (C57/BL6 background) were a gift from Andreas Zimmer, University of Bonn, Germany. All animals were housed under standard conditions. Approval for animal experimentation was granted before by the Regional Government of

Lower Franconia, Würzburg, Germany (No. 54-2531.31-18/06).

Fibrosis was induced by a modified protocol of 3 \times /wk intraperitoneal (i.p.) application of 0.15 mg/kg TAA and continuous feeding of 10% (v/v) ethanol (EtOH) in sweetened drinking water for 18 wks (26). Untreated control groups received regular food and water *ad libitum*. Each of the four experimental groups consisted of eight animals.

Animals were killed by cervical dislocation and liver samples were snap frozen in liquid nitrogen for isolation of mRNA and protein, or fixed in 4%

phosphate-buffered formalin for paraffin embedding. Regular hematoxylin and eosin (H&E) staining was performed to evaluate standard histomorphology of liver tissues and to assess the grade of inflammation. Sirius red staining was used to visualize fibrosis.

Quantitative Real-Time PCR

Total RNA was isolated from snap frozen tissues or from semiconfluent cells using the RNeasy kit (Qiagen, Basel, Switzerland) and converted to cDNA as described (27). Quantitative real-time PCR was performed on a Bio-Rad CFX96 system (Bio-Rad Laboratories, Munich, Germany) and on the ABI 7700 Sequence Detector (Applied Biosystems, Rotkreuz, Switzerland) using QuantiTect Primers (Qiagen, Hilden, Germany) and the LightCycler FastStart DNA Master SYBR Green I kit (Roche Molecular Diagnostics, Basel, Switzerland). For normalization, the housekeeping gene *glyceraldehyde 3-phosphate dehydrogenase (GAPDH)* was amplified in a parallel reaction. Sequences of primers and probes are summarized in Supplementary Table 1.

Hepatic Hydroxyproline

Hepatic hydroxyproline (HYP) was measured as described previously (27, 28). Briefly, liver tissues (200 mg) were hydrolyzed in 6 mol/L HCl at 110°C for 16 h. Fifty microliters of each sample was incubated with chloramine T (2.5 mmol/L) for 5 min and Ehrlich's reagent (410 mmol/L) for 30 min at 60°C. Absorption was measured in triplicates at 560 nm. Results are expressed as $\mu\text{g/g}$ of wet liver tissue.

Cell Culture Experiments

Human HSC, isolated from resected human livers (kindly donated by M Pinzani, Florence, Italy) (29,30) and moderately activated rat HSC cell line CFSC-2G, isolated from cirrhotic rat livers (29,31,32) (generously provided by M Rojkind, Washington DC, USA) were cultured in DMEM containing 10% FBS, 2 mmol/L glutamine, 100 U/mL penicillin and 100 U/mL streptomycin. Cells

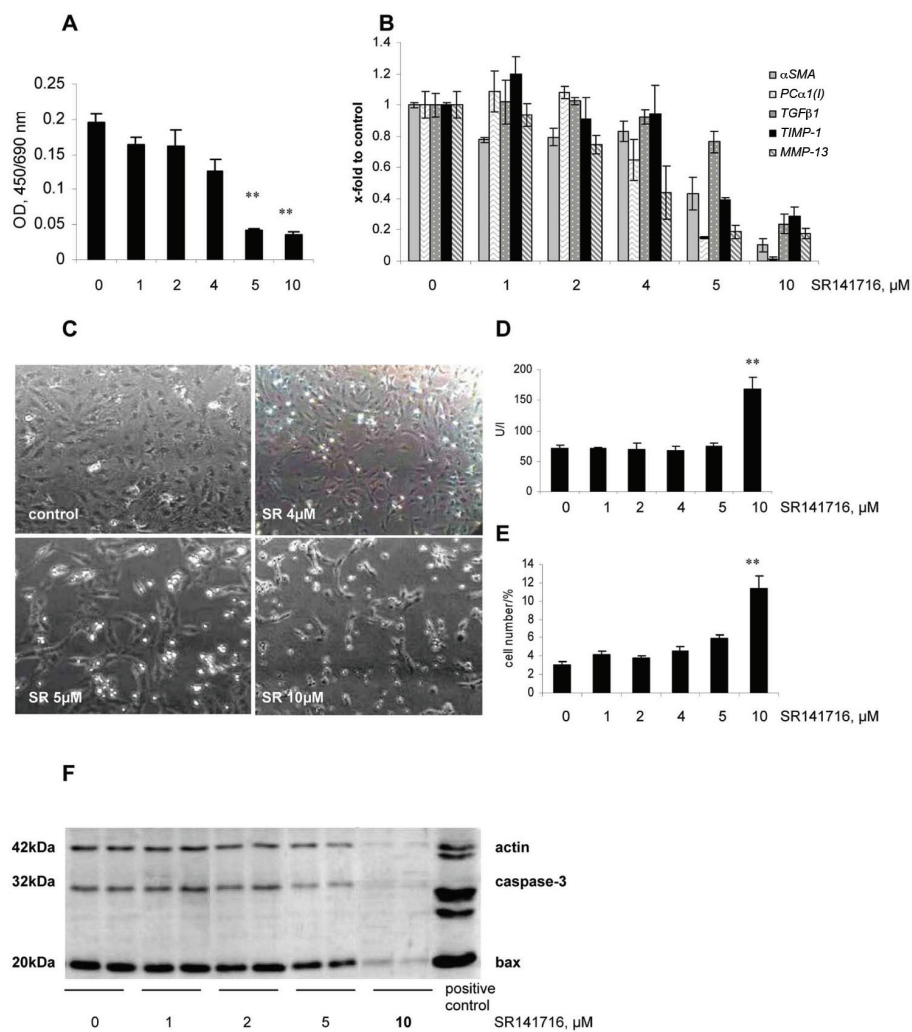


Figure 3. The effect of SR141716 on HSC proliferation, gene expression and apoptosis. (A) DNA synthesis, assessed by BrdU incorporation after 48 h treatment with SR141716; (B) *αSMA*, *PCα1(I)*, *TGFβ1*, *TIMP-1*, *MMP-13* mRNA expression, measured by TaqMan PCR and normalized to *GAPDH*. Cell toxicity of (C) SR141716 (magnification 10x), evaluated by (D) LDH leakage, (E) Trypan Blue stain, and apoptosis markers caspase-3 (cleaved and total) and (F) bax, measured by Western blotting after 48 h treatment with SR141716 (mean ± SD; **P* < 0.05, ***P* < 0.005).

were maintained at 37°C in a 5% CO₂ humidified atmosphere.

For all experiments, cells were seeded onto 6- or 12-well plates and, after reaching semiconfluent conditions, starved in serum-free DMEM for 24 h. Treatment with AA (Fluka, Buchs, Switzerland; 200 μmol/L), H₂O₂ (1–50 μmol/L), 2-AG (Sigma-Aldrich, Munich, Germany; 1–20 μmol/L), THC (200–1000 nmol/L) or SR141716/rimonabant (Sanofi-Aventis SA, Paris, France; 100 nm to 10 μmol/L)

was performed for 6 to 48 h under normoxic (24% O₂) or hypoxic (1% O₂) conditions using a hypoxia workstation (Ruskin Technology Limited, West Yorkshire, UK).

Cell Viability Analysis

Cells were seeded at 6 × 10⁴ onto 6-well culture plates, and, after reaching semiconfluent state, starved in serum-free DMEM, and treated with different compounds for the following 24 to 48 h.

Trypan blue-excluding cells were counted under a light microscope.

For LDH analysis, the supernatants from both the untreated and the treated cells were collected and LDH leakage was assayed with a standard kit (Diatools AG, Villmergen, Switzerland) and an autoanalyzer (Olympus Autoanalyzer AU 2700, Kobe, Japan).

BrdU Incorporation or DNA Synthesis

Cells were seeded at a density of 5 × 10⁴ per well in 96-well plates and after 24 h of starvation, tested compounds were applied for the next 24 h. BrdU was added during the last 4 h and the amount of BrdU incorporation was determined by a colorimetric BrdU cell proliferation enzyme-linked immunoassay (ELISA) according to the manufacturer’s instructions (Roche, Mannheim, Germany). All experiments were done with 6 wells per group and repeated at least three times.

Western Blot Analysis

Protein extracts from liver tissue samples were separated by SDS-PAGE, proteins transferred and membranes probed with mouse monoclonal anti-caspase-3 (cleaved and total), anti-bax and anti-actin antibodies (Cell Signaling Technology Inc., Danvers, MA, USA), followed by incubation with horseradish peroxidase-conjugated goat anti-mouse antibody (Pierce, Rockford, IL, USA). Signals were detected with enhanced chemiluminescence (Western Lightning Chemiluminescence Reagent Plus, Perkin-Elmer Life Science, Boston, MA, USA), imaged and quantified using AIDA software (Raytest, Urdorf, Switzerland).

Immunohistochemistry

Specimens were deparaffinized and antigen retrieval performed by boiling in sodium citrate buffer (pH 6.0) for 15 min and in 0.1% Trypsin for 20 min at 37°C. After blocking of endogenous peroxidase by 0.6% H₂O₂ and unspecific binding by 2% goat serum, primary rabbit polyclonal anti-CB1 (Abcam, Cambridge, UK) or anti-CB2 antibody (Novus Biologicals, Littleton, CO, USA) were applied (1:300) and incu-

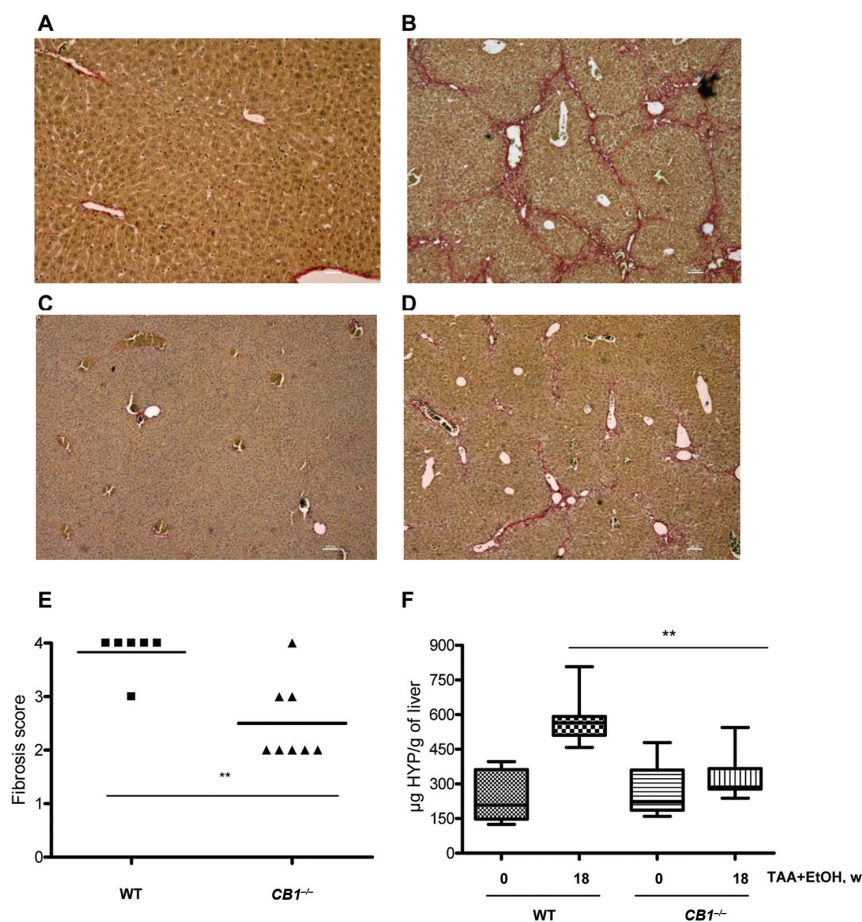


Figure 4. Histology and liver collagen accumulation in wild-type and *CB1*^{-/-} mice after fibrosis induction. (A) wild-type (WT) control; (B) WT + TAA/EtOH treatment, 18 wks; (C) *CB1*^{-/-} control; (D) *CB1*^{-/-} + TAA/EtOH treatment, 18 wks. Fibrotic septa are clearly visible on tissues of WT alcohol-treated mice (red color), whereas only minor fibrosis is found in *CB1*^{-/-} mice following TAA/EtOH treatment. Shown are representative images (magnification 10×). Fibrosis stages after 18 wks of TAA/EtOH (E) and relative HYP (F), µg/g of wet liver (mean ± SD; ***P* < 0.005).

bated overnight at 4°C, followed by biotinylated goat anti-mouse secondary antibody (1:350) for 1 h at room temperature. Detection with diaminobenzidine (DAKO, Glostrup, Denmark) was performed after incubation with HRP-streptavidin solution (Vector Labs, Burlingame, VT, USA). Nuclei were stained with Mayer's Hematoxylin. Histopathological evaluations were performed in a blinded fashion by two investigators (E Patsenker and F Stickel).

Statistical Analysis

Statistical analyses were performed using Microsoft EXCEL software. Data

are expressed as mean ± SD. The statistical significance of differences was evaluated using the unpaired Student *t* test or nonparametric analysis of variance (ANOVA) Kruskal-Wallis test.

All supplementary materials are available online at www.molmed.org.

RESULTS

CB1 and *CB2* Expression in Human ALD

Immunohistochemistry of sections from patients with ALD showed restric-

tion of *CB1* to fibrotic septa, whereas the liver parenchyma was found entirely negative (Figures 1A, B). *CB2* IHC turned out negative regardless of the stage of fibrosis (not shown). At the mRNA level, *CB1* and *procollagen (PC) α1(I)* were significantly induced with fibrosis progression (Figures 1C, D), while *CB2* mRNA levels were not significantly different between fibrosis stages (Figure 1E).

CB1 Is Upregulated by Acetaldehyde in HSC

In human HSC, *CB1* mRNA was significantly and dose-dependently induced by acetaldehyde (AA) with a two-fold increase at the highest concentration of 200 µmol/L after 24 h, whereas the difference was not significant after 6 h (Figure 2A). *CB2* mRNA transcripts were not affected significantly by AA at any concentration or time point (Figure 2B). Interestingly, well-known mediators of alcohol-induced liver injury such as reactive oxygen species and hypoxia showed opposing effects on *CB1* expression; while treatment with H₂O₂ dose-dependently induced *CB1* mRNA up to three-fold at 50 µmol/L, this was reduced three-fold under highly hypoxic conditions (Figures 2C, D).

Treatment of rat HSC with THC or 2-AG dose-dependently upregulated *CB1* mRNA (not shown), reaching almost two-fold induction at 1 µmol/L and 20 µmol/L, respectively, after 24 h. Moreover, combination of THC or 2-AG with AA further increased the expression of *CB1* five- and three-fold, respectively, compared with THC or 2-AG alone (Figure 2E).

In addition, the marker of HSC activation, *αSMA*, was strongly induced by 2-AG alone, and in combination with AA by 40% and 100%, respectively (Figure 2F), whereas other fibrosis-associated genes such as *PCα1(I)*, *TGFβ1* and *TIMP-1* were not affected by THC or 2-AG during the observation interval (data not shown). Notably, there were no toxic or apoptotic effects by AA alone or in combination with 2-AG and THC, as

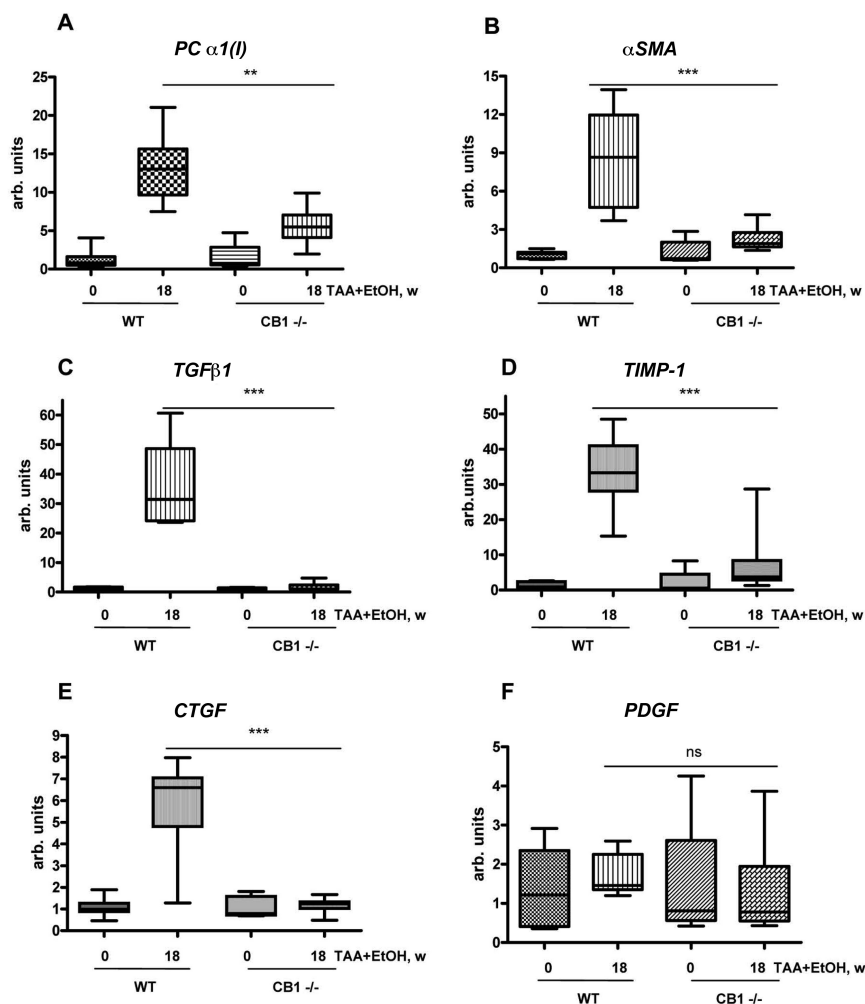


Figure 5. Fibrosis-related mRNA in wild-type and *CB1*^{-/-} mice after fibrosis induction. (A) *PCα1(I)*, (B) *αSMA*, (C) *TGFβ1*, (D) *TIMP-1*, (E) *CTGF* and (F) *PDGF* mRNA after 18 wks of treatment with/without TAA/EtOH; measured by TaqMan PCR and normalized to *GAPDH* (mean ± SD; **P* < 0.05, ***P* < 0.005, ****P* < 0.0005; ns, not significant).

shown by LDH leakage (Supplementary Figure 1A), Trypan Blue stain (not shown) or proapoptotic caspase-3 activation, in spite of bax activation in presence of 1 μmol/L THC (Supplementary Figure 1C). Slight, but not significant inhibition of rat HSC proliferation by AA and THC also was observed (Supplementary Figure 1B).

The effect of ethanol (EtOH) itself was tested in the same experimental setting. However, there was no significant effect found on *CB1* mRNA, *PCα1(I)* or *αSMA* mRNA in rat HSC using 10–200 mmol/L EtOH (Supplementary Figure 2), whereas

at 300–500 mmol/L it revealed toxicity (not shown).

SR141716/Rimonabant Exerts Toxicity on HSC

Effects of SR141716 on rat HSC at concentrations below 1 μmol/L showed no effect on any cellular functions tested (data not shown). However, DNA synthesis was inhibited approximately four-fold by both 5 and 10 μmol/L (Figure 3A), and mRNA expression for *αSMA*, *PCα1(I)*, *TIMP-1* and *MMP-13* was downregulated by more than 50% by 5 and 10 μmol/L (Figure 3B). Analysis of

cell death revealed significant toxicity of SR141716 at 10 μmol/L after 48 h of incubation (Figure 3C), which was confirmed by LDH leakage and Trypan Blue staining (Figures 3D, E). Notably, neither total caspase-3, nor bax were induced by SR141716, but rather decreased due to toxic effects (Figure 3F) ruling out significant proapoptotic effects from SR141716 on HSC. Similarly, Bcl-2 and cleaved caspase-3 were not induced in any of the groups (data not shown).

***CB1*^{-/-} Mice Are Resistant to Alcohol-Induced Liver Fibrosis**

Eighteen wks of TAA/EtOH administration caused significant fibrosis with accumulation of collagen fibers in pericentral areas, leading to micronodular cirrhosis in WT mice, whereas *CB1*^{-/-} mice showed a markedly lesser extent of hepatic collagen deposition (Figures 4A–D). Evaluation of fibrosis stage (Figure 4E) and quantification of fibrosis by measuring relative HYP confirmed significantly reduced collagen levels in *CB1*^{-/-} mice versus WT mice (Figure 4F).

The expression of *PC α1(I)*, *αSMA*, *TGFβ1*, *TIMP-1*, *CTGF* and *PDGF* was strongly affected by TAA/EtOH with all (except for *PDGF*) of the measured mRNA transcripts being upregulated significantly in WT mice, whereas *CB1*^{-/-} mice had much lower levels (*P* < 0.005) (Figures 5A–F).

Interestingly, TAA/EtOH affected the expression of *matrix metalloproteinases* (*MMP*)-2 and -3 in WT mice and in *CB1*^{-/-} mice strikingly, resulting in significantly lower expression levels in *CB1*^{-/-} mice (Figures 6A, B). For *MMP-9* and *MMP-13*, differences between treated groups did not reach statistical significance although there was a trend toward higher expression in *CB1*^{-/-} mice treated with TAA/EtOH (Figures 6C, D).

Hepatic Inflammation Is Mildly Affected in *CB1*^{-/-} Mice upon Fibrosis Induction

Portal and lobular inflammation was estimated from histologic liver sections (Figures 7A, B) and showed no or minor

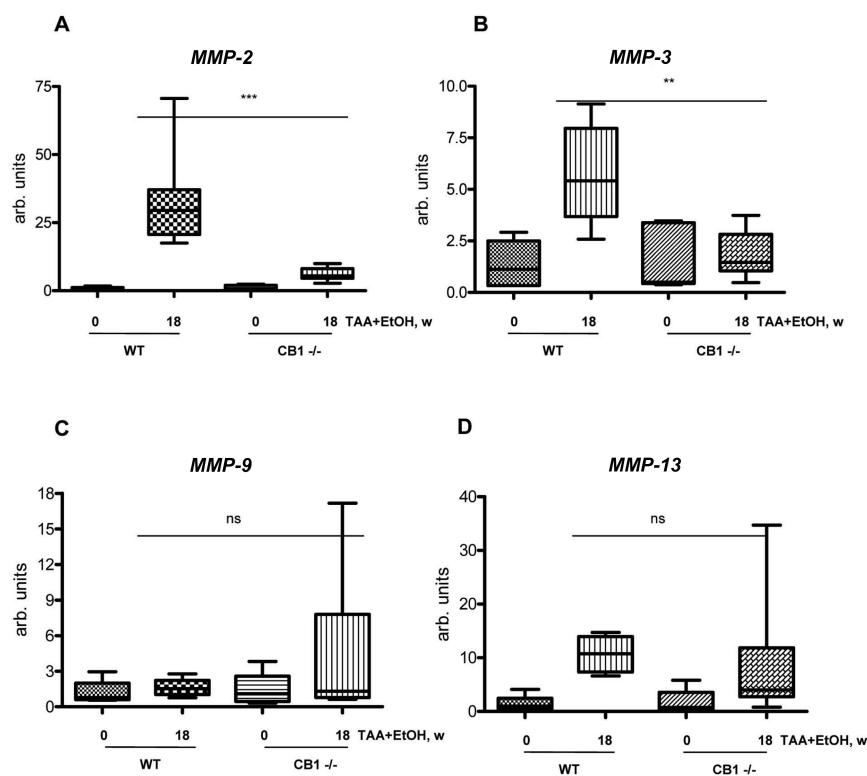


Figure 6. Matrix metalloproteinases mRNA in wild-type and *CB1*^{-/-} mice after fibrosis induction. (A) *MMP-2*, (B) *MMP-3*, (C) *MMP-9* and (D) *MMP-13* mRNA after 18 wks of treatment with/without TAA/EtOH; measured by TaqMan PCR and normalized to *GAPDH* (mean \pm SD; * P < 0.05, ** P < 0.005, *** P < 0.0005; ns, not significant).

lobular inflammation in both WT and *CB1*^{-/-} mice receiving TAA/EtOH, whereas portal inflammatory activity was significant, but slightly less pronounced in *CB1*^{-/-} mice as compared with WT mice (Figure 7C).

Expression of genes coding for surrogate markers of inflammation including *COX-2*, *iNOS* and *TNF α* were significantly upregulated by TAA/EtOH in WT animals. In *CB1*^{-/-} mice, *iNOS* and *TNF α* expression also were moderately increased by TAA/EtOH treatment, whereas *COX-2* expression remained unaffected (Figures 7D–F).

DISCUSSION

The significance of ECS in modulating fibrosis, steatosis and cell regeneration in experimental liver injury has been demonstrated and reviewed (7,8,33), and CB receptors are induced in acute and chronic liver injury including cirrhosis

(14). However, its involvement in alcoholic liver fibrosis was unknown until the present study, which describes the engagement of ECS in the evolution of alcohol-induced liver fibrosis by showing the expression of *CB1* in human ALD, its induction in HSC upon challenge with acetaldehyde and reactive oxygen species and a marked resistance of *CB1*^{-/-} mice toward chronic liver injury modulated further by alcohol. Upregulation of *CB1* in human cirrhosis was described by Lotersztajn *et al.* (9), however, in their study, only four patients with alcoholic cirrhosis were included. Also, no patients with precirrhotic alcoholic liver injury were studied. Interestingly, *CB2* expression was not detectable in our study on protein level in humans, further, it remained unaffected by alcohol at mRNA level, and did not correlate with the severity of fibrosis. These findings were confirmed *in vitro*, demonstrating the

same expression pattern for *CB1* and *CB2* from human HSC. An increased *CB2* expression by HSC during activation in culture was shown by Julien *et al.* (10) but specific treatment of fully activated HSC with alcohol did not have the same effect. Therefore, we hypothesize that there exists an induction of “profibrogenic” *CB1* paralleled by an unchanged expression of “antifibrogenic” *CB2* which then swings the balance toward net matrix accumulation rather than its degradation.

Endocannabinoid levels, such as of 2-AG and AEA are increased in liver disease (14–16,20). Here, we show that 2-AG and THC induce *CB1* mRNA, which is further enhanced by their combination with AA, jointly favoring the progression of fibrosis in ALD. Moreover, combination of AA and 2-AG resulted in an even stronger upregulation of α SMA in HSC than treatment with either 2-AG or AA alone, indicating its high activation potential. Interestingly, there was no indication of apoptosis following treatment with THC or 2AG at the doses applied, which conflicts with some of the published data from Julien *et al.* (10) who demonstrated that THC at 1–4 μ mol/L and 2-AG at 20 μ mol/L exert antiproliferative and proapoptotic effects. However, in the same study, no effect on cell viability by THC at 1 μ mol/L in the presence of PDGF was shown. So, it can be concluded that cellular responses toward potentially proapoptotic stimuli are variable and depend on the conditions used. In addition, cell-specific differences between primary and immortalized cells should be taken into account.

The *CB1* antagonist SR141716 revealed potent antifibrotic properties at 5 μ mol/L without causing significant cell death, before exerting cytotoxic properties on HSC when applied at doses from 5 to 10 μ mol/L.

Our data clearly show that *CB1*^{-/-} mice do not develop liver fibrosis after 18 wks of TAA/EtOH administration. All surrogate markers of fibrosis, such as extracellular matrix deposition, hydroxyproline and mRNA levels of fibrosis-mediating genes consistently demonstrate that

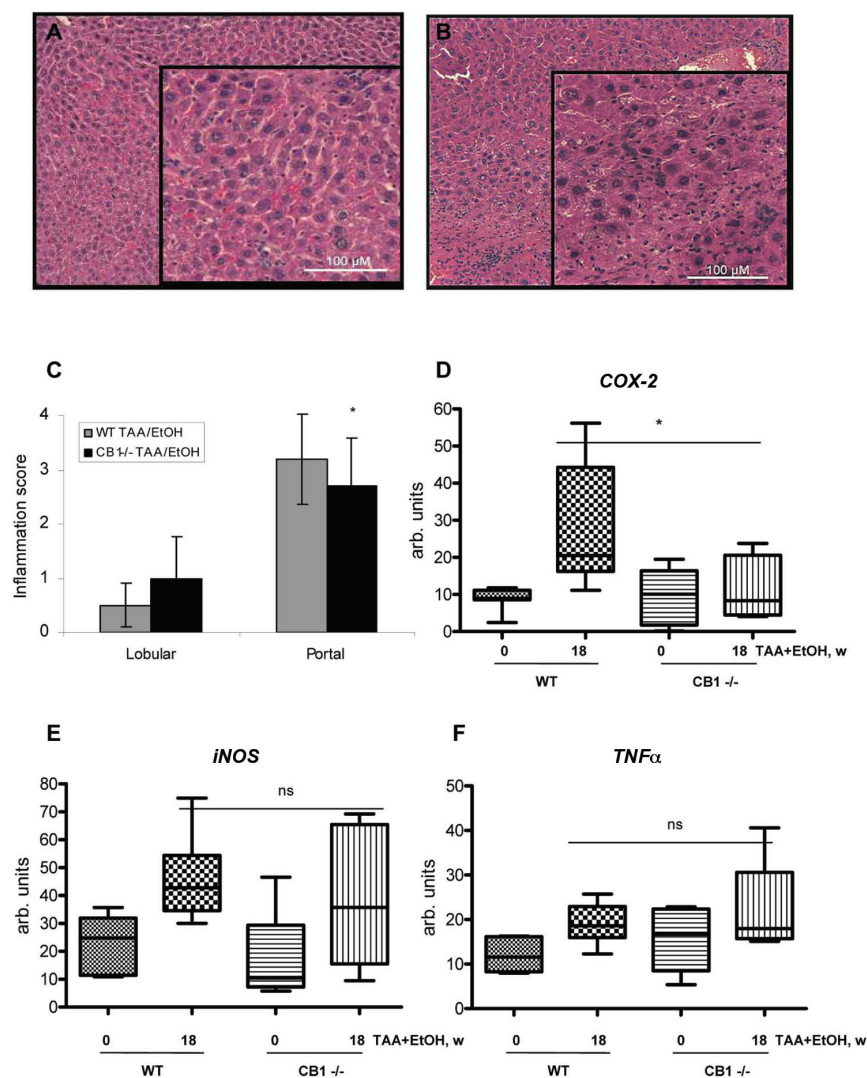


Figure 7. Hepatic inflammation in wild-type and *CB1*^{-/-} mice after fibrosis induction. Portal and lobular inflammation in (A) WT and (B) *CB1*^{-/-} mice after 18 wks of TAA/EtOH administration, evaluated from H&E staining and presented as inflammation score (C) (mean ± SD; **P* < 0.05 versus WT). (D) *COX-2*, (E) *iNOS* and (F) *TNFα* mRNA after 18 wks with/without TAA/EtOH; measured by TaqMan PCR and normalized to *GAPDH* (mean ± SD; **P* < 0.05; ns, not significant).

CB1^{-/-} mice are effectively protected from fibrosis development. One of the mechanisms for resolution of hepatic fibrosis could be the activation of matrix metalloproteinases, such as interstitial collagenases (human MMP-1/murine MMP-13), stromelysin-1 (MMP-3), and gelatinases A and B (MMP-2 and MMP-9, respectively) which degrade matrix molecules and may contribute to fibrolysis and fibrosis resolution (34–36). We found a

strong upregulation of *MMP-2*, *-3* and *-13* in WT mice compared with *CB1*^{-/-} animals. This seemingly contradictory observation with regards to the balance between fibrogenesis and fibrolysis can be explained by the very complex and different regulation of *MMP* expression and enzymatic activation during the peak of fibrosis formation and ECM degradation (34,37). Certain *MMPs*, such as profibrogenic *MMP-2*, facilitate and promote

degradation of basement membrane with subsequent activation, migration and proliferation of HSC/myofibroblasts, resulting in progression of liver injury and fibrosis (38), whereas others, such as *MMP-3*, *-9* and *-13* participate in the degradation of extracellular matrix and fibrosis resolution (35,39). In our study, the induction of fibrolytic *MMP-3* and *-13* in parallel with *MMP-2* may reflect a fibrolytic response in an attempt to degrade excessive matrix, which, however, is not sufficient to overcome the profibrogenic stimuli from the toxic treatment in WT mice. In *CB1*^{-/-} mice induction of *MMPs* was not so prominent with less induced *MMP-2* and elevated *MMP-9* and *-13*, indicating a shift toward enhanced fibrolysis.

Several publications described the involvement of the ECS in hepatic inflammation. In spite of the primary role of the CB2 receptor, CB1 also has been shown to be involved in inflammatory processes (33). Thus, CB1 was found expressed in almost all human peripheral blood immune cells, including B lymphocytes, natural killer cells, polymorphonuclear neutrophils, CD8 and CD4 lymphocytes and monocytes (40). In experimental models of liver fibrosis, both CB2 receptor agonists and CB1 receptor antagonists exerted variable effects via different mechanisms which may involve modulation of the secondary inflammatory response (5,8). A recent study suggested that an antiinflammatory effect of CB1 antagonist SR141716 also may contribute to the favorable effects of CB1 receptor antagonists in the treatment of obesity, nonalcoholic fatty liver disease and closely related features of the metabolic syndrome (41). However, published data in this regard remain contradictory, and only one study addressed the mechanisms of how the ECS intercepts with inflammatory processes (23). In our study, we observed moderately reduced portal inflammation and a lack of *COX-2* upregulation in *CB1*^{-/-} mice following alcohol exposure, while *TNFα* and *iNOS* were not different between *CB1*^{-/-} and WT

mice, suggesting that the absence of *CB1* has little impact on well-established triggers of hepatic inflammation.

Two aspects of our experimental set up make it difficult to draw direct conclusions for human ALD: (a) the experimental model we used is certainly not perfect in mimicking ALD in human, but a reliable experimental model for inducing liver fibrosis in mice. Kornek *et al.* have clearly shown, that the addition of alcohol TAA further increases liver injury compared with TAA alone, although features of ALD such as steatosis, Mallory bodies, and “chicken-wire fibrosis” were missing (26). However, rodents are known to be notoriously resistant to fibrosis induction, and most models require addition of a second fibrosis trigger to alcohol administration (26,42); (b) the acetaldehyde concentration of 200 $\mu\text{mol/L}$ causing significant *CB1* up-regulation in our study is approximately two-fold higher than hepatic concentrations typically encountered in human ALD, but still in the order of what has been described in experimental ALD after dosing rats with different amounts of alcohol (43–46).

In conclusion, induction of *CB1* receptor by AA due to chronic alcohol exposure, as well as by either endo- or exocannabinoids, and, more strikingly, by their combination, are suggestive of a relevant involvement of the ECS in the evolution of ALD, and suggest additive effects of concomitant cannabis consumption in individuals who consume excess alcohol, and may point to *CB1* antagonism for treatment of fibrotic ALD, particularly, as *CB1* antagonists have been used in treating alcohol dependence without causing significant depression (47) as was observed in patients with nonalcoholic fatty liver disease (48).

ACKNOWLEDGMENTS

We are most grateful to Andreas Zimmer from the University of Bonn, Germany, for providing access to the *CB1*^{-/-} mice. This work was supported by grant 3100 A0 -122114/1 from the Swiss National Science Foundation and by the Eu-

ropean Research Advisory Board (ERAB; grant EA 09 20). MO was supported by a grant of the von-Behring-Röntgen Foundation, Marburg, Germany. HKS received funding from the Manfred Lautenschläger Foundation, Heidelberg, Germany.

DISCLOSURE

The authors declare that they have no competing interests as defined by *Molecular Medicine*, or other interests that might be perceived to influence the results and discussion reported in this paper.

REFERENCES

- Bataller R, Brenner DA. (2005) Liver fibrosis. *J. Clin. Invest.* 115:209–18.
- Bataller R, Brenner DA. (2001) Hepatic stellate cells as a target for the treatment of liver fibrosis. *Semin. Liver Dis.* 21:437–51.
- Parsons CJ, Takashima M, Rippe RA. (2007) Molecular mechanisms of hepatic fibrogenesis. *J. Gastroenterol. Hepatol.* 22 Suppl 1:S79–84.
- Friedman SL. (2008) Mechanisms of hepatic fibrogenesis. *Gastroenterology.* 134:1655–69.
- Mallat A, Teixeira-Clerc F, Deveaux V, Lotersztajn S. (2007) Cannabinoid receptors as new targets of antifibrotic strategies during chronic liver diseases. *Expert Opin. Ther. Targets* 11:403–9.
- Caraceni P, Domenicali M, Bernardi M. (2008) The endocannabinoid system and liver diseases. *J. Neuroendocrinol.* 20 Suppl 1:47–52.
- Parfieniuk A, Flisiak R. (2008) Role of cannabinoids in chronic liver diseases. *World J. Gastroenterol.* 14:6109–14.
- Siegmund SV, Schwabe RF. (2008) Endocannabinoids and liver disease. II. Endocannabinoids in the pathogenesis and treatment of liver fibrosis. *Am. J. Physiol. Gastrointest. Liver Physiol.* 294:G357–62.
- Teixeira-Clerc F, *et al.* (2006) *CB1* cannabinoid receptor antagonism: a new strategy for the treatment of liver fibrosis. *Nat. Med.* 12:671–6.
- Julien B, *et al.* (2005) Antifibrotic role of the cannabinoid receptor *CB2* in the liver. *Gastroenterology.* 128:742–55.
- Ishida JH, *et al.* (2008) Influence of cannabis use on severity of hepatitis C disease. *Clin. Gastroenterol. Hepatol.* 6:69–75.
- Hezode C, *et al.* (2005) Daily cannabis smoking as a risk factor for progression of fibrosis in chronic hepatitis C. *Hepatology.* 42:63–71.
- Hezode C, *et al.* (2008) Daily cannabis use: a novel risk factor of steatosis severity in patients with chronic hepatitis C. *Gastroenterology.* 134:432–9.
- Caraceni P, *et al.* (2009) Circulating and hepatic endocannabinoids and endocannabinoid-related molecules in patients with cirrhosis. *Liver Int.* 30:816–25.

- Biswas KK, *et al.* (2003) Membrane cholesterol but not putative receptors mediates anandamide-induced hepatocyte apoptosis. *Hepatology.* 38:1167–77.
- Osei-Hyiaman D, *et al.* (2005) Endocannabinoid activation at hepatic *CB1* receptors stimulates fatty acid synthesis and contributes to diet-induced obesity. *J. Clin. Invest.* 115:1298–305.
- Siegmund SV, *et al.* (2006) Fatty acid amide hydrolase determines anandamide-induced cell death in the liver. *J. Biol. Chem.* 281:10431–8.
- Maccarrone M, Finazzi-Agro A. (2003) The endocannabinoid system, anandamide and the regulation of mammalian cell apoptosis. *Cell Death Differ.* 10:946–55.
- Siegmund SV, Uchinami H, Osawa Y, Brenner DA, Schwabe RF. (2005) Anandamide induces necrosis in primary hepatic stellate cells. *Hepatology.* 41:1085–95.
- Siegmund SV, *et al.* (2007) The endocannabinoid 2-arachidonoyl glycerol induces death of hepatic stellate cells via mitochondrial reactive oxygen species. *FASEB J.* 21:2798–806.
- Jeong WI, *et al.* (2008) Paracrine activation of hepatic *CB1* receptors by stellate cell-derived endocannabinoids mediates alcoholic fatty liver. *Cell Metab.* 7:227–35.
- Trebicka J, *et al.* (2011) Role of cannabinoid receptors in alcoholic hepatic injury: steatosis and fibrogenesis are increased in *CB2* receptor-deficient mice and decreased in *CB1* receptor knockouts. *Liver Int.* 31:860–70.
- Louvet A, *et al.* (2011) Cannabinoid *CB2* receptors protect against alcoholic liver disease by regulating Kupffer cell polarization in mice. *Hepatology.* doi: 10.1002/hep.24524. [Epub ahead of print].
- Siegmund SV, Haas S, Singer MV (2005) Animal models and their results in gastrointestinal alcohol research. *Dig. Dis.* 23:181–94.
- Kleiner DE, *et al.* (2005) Design and validation of a histological scoring system for nonalcoholic fatty liver disease. *Hepatology.* 41:1313–21.
- Kornek M, *et al.* (2006) Combination of systemic thioacetamide (TAA) injections and ethanol feeding accelerates hepatic fibrosis in C3H/He mice and is associated with intrahepatic up-regulation of MMP-2, VEGF and ICAM-1. *J. Hepatol.* 45:370–6.
- Patsenker E, *et al.* (2008) Inhibition of integrin $\alpha\text{phv}\beta\text{6}$ on cholangiocytes blocks transforming growth factor- β activation and retards biliary fibrosis progression. *Gastroenterology.* 135:660–70.
- Patsenker E, *et al.* (2009) Pharmacological inhibition of integrin $\alpha\text{phv}\beta\text{3}$ aggravates experimental liver fibrosis and suppresses hepatic angiogenesis. *Hepatology.* 50:1501–11.
- Patsenker E, Popov Y, Wiesner M, Goodman SL, Schuppan D. (2007) Pharmacological inhibition of the vitronectin receptor abrogates PDGF-BB-induced hepatic stellate cell migration and activation in vitro. *J. Hepatol.* 46:878–87.
- Faillit P, *et al.* (1995) The mitogenic effect of

- platelet-derived growth factor in human hepatic stellate cells requires calcium influx. *Am. J. Physiol.* 269:C1133-9.
31. Inagaki Y, et al. (1995) Regulation of the alpha 2(I) collagen gene transcription in fat-storing cells derived from a cirrhotic liver. *Hepatology.* 22:573-9.
 32. Rojkind M, et al. (1995) Characterization and functional studies on rat liver fat-storing cell line and freshly isolated hepatocyte coculture system. *Am. J. Pathol.* 146:1508-20.
 33. Pacher P, Gao B. (2008) Endocannabinoids and liver disease. III. Endocannabinoid effects on immune cells: implications for inflammatory liver diseases. *Am. J. Physiol. Gastrointest. Liver Physiol.* 294:G850-4.
 34. Benyon RC, Arthur MJ. (2001) Extracellular matrix degradation and the role of hepatic stellate cells. *Semin. Liver Dis.* 21:373-84.
 35. Fallowfield JA, et al. (2007) Scar-associated macrophages are a major source of hepatic matrix metalloproteinase-13 and facilitate the resolution of murine hepatic fibrosis. *J. Immunol.* 178:5288-95.
 36. Winwood PJ, et al. (1995) Kupffer cell-derived 95-kd type IV collagenase/gelatinase B: characterization and expression in cultured cells. *Hepatology.* 22:304-15.
 37. Popov Y, et al. Macrophage-mediated phagocytosis of apoptotic cholangiocytes contributes to reversal of experimental biliary fibrosis. *Am. J. Physiol. Gastrointest. Liver Physiol.* 298:G323-34.
 38. Olaso E, et al. (2001) DDR2 receptor promotes MMP-2-mediated proliferation and invasion by hepatic stellate cells. *J. Clin. Invest.* 108:1369-78.
 39. Popov Y, Patsenker E, Fickert P, Trauner M, Schuppan D. (2005) Mdr2 (Abcb4)-/- mice spontaneously develop severe biliary fibrosis via massive dysregulation of pro- and antifibrogenic genes. *J. Hepatol.* 43:1045-54.
 40. Klein TW, et al. (2003) The cannabinoid system and immune modulation. *J. Leukoc. Biol.* 74:486-96.
 41. Gary-Bobo M, et al. (2007) Rimonabant reduces obesity-associated hepatic steatosis and features of metabolic syndrome in obese Zucker fa/fa rats. *Hepatology.* 46:122-9.
 42. Chen YH, Wang MF, Liao JW, Chang SP, Hu ML. (2008) Beneficial effects of nicotinamide on alcohol-induced liver injury in senescence-accelerated mice. *Biofactors.* 34:97-107.
 43. Brenner DA, Chojkier M. (1987) Acetaldehyde increases collagen gene transcription in cultured human fibroblasts. *J. Biol. Chem.* 262:17690-5.
 44. Eriksson CJ, Sippel HW. (1977) The distribution and metabolism of acetaldehyde in rats during ethanol oxidation-I. The distribution of acetaldehyde in liver, brain, blood and breath. *Biochem. Pharmacol.* 26:241-7.
 45. Chen A. (2002) Acetaldehyde stimulates the activation of latent transforming growth factor-beta1 and induces expression of the type II receptor of the cytokine in rat cultured hepatic stellate cells. *Biochem. J.* 368:683-93.
 46. Siegmund SV, Dooley S, Brenner DA. (2005) Molecular mechanisms of alcohol-induced hepatic fibrosis. *Dig. Dis.* 23:264-74.
 47. Soyka M, et al. (2008) Cannabinoid receptor 1 blocker rimonabant (SR 141716) for treatment of alcohol dependence: results from a placebo-controlled, double-blind trial. *J. Clin. Psychopharmacol.* 28:317-24.
 48. European Medicines Agency. (2008) The European Medicines Agency recommends suspension of the marketing authorisation of Acomplia [press release]. [cited 2011 Oct 28]. Available from: http://www.ema.europa.eu/ema/index.jsp?curl=pages/news_and_events/news/2009/11/news_detail_000244.jsp&murl=menus/news_and_events/news_and_events.jsp&mid=WC0b01ac058004d5c1&jsenabled=true